JWMM

A Bio-inspired and Deep Learning Based Hybrid Model for Agricultural Drought Assessment

Shilpa Chaudhari, Aniketh Anchalia, Anirudh Kakati, Ankit Paudel, Bhavana BN, and Vandana Sardar (2024)

M.S. Ramaiah Institute of Technology, Bangalore, India

DOI: https://doi.org/10.14796/JWMM.C512

ABSTRACT

Agricultural droughts can cause many serious hazards. Drought monitoring indices, namely Normalized Difference Vegetation Index (NDVI), Atmospherically Resistant Vegetation Index (ARVI), Soil Adjusted Vegetation Index (SAVI), and Enhanced Vegetation Index (EVI) have been used for an agricultural drought assessment. Satellite images from the Kolar region of Karnataka are used to calculate these indices. This paper proposes an integration model based on Convolutional Neural Networks (CNN) and a bio-inspired algorithm (Sparrow Search Algorithm (SSA) and Barnacles Mating Optimizer (BMO)) considering the indices as population. Performance is compared with the standalone CNN model in terms of efficiency. For the CNN, the accuracy, time taken for Epoch1, and time taken for Epoch2 is 91%, 16s (3s/step), and 2s (2s/step), respectively. For the CNN integrated with SSA, it is 94%, 3s (3s/step) and 0s (43ms/step), respectively. For the CNN integrated with BMO, it is 94%, 3s (2s/step) and 0s (46ms/step) respectively.

1. INTRODUCTION

All types of droughts can have negative effects on society, but agricultural drought is particularly dangerous for both consumers and animal producers. Insufficient precipitation causes droughts. Agriculture predominates in most rural areas of Karnataka, where temperatures are unusually hot and there is a dearth of precipitation. The results of previous pattern analysis through early warning drought monitoring and

Chaudhari, S., A. Anchalia, A. Kakati, A. Paudel, B. BN, and V. Sardar. 2024. "A Bio-inspired and Deep Learning Based Hybrid Model for Agricultural Drought Assessment." *Journal of Water Management Modeling* 32: C512. https://doi.org/10.14796/JWMM.C512 www.chijournal.org ISSN: 2292-6062

forecasting upcoming drought conditions aid in reducing or controlling the causes of drought in several industries. Many drought indices, such as the Normalized Difference Vegetation Index (NDVI), Vegetation Condition Index (VCI), Temperature Condition Index (TCI), Atmospherically Resistant Vegetation Index (ARVI), Landsat Enhanced Vegetation Index (EVI), Standardized Precipitation Index (SPI), Soil Adjusted Vegetation Index (SAVI), etc., are useful for monitoring and predicting agricultural drought. Typical techniques that rely on meteorological point data being available, such as rainfall amount and subsequently the accompanying indices, have been used by most drought prediction techniques.

Among the most frequent ways to conduct remote sensing in agriculture is through satellites. These objects stand in for actual geographic conditions like drought or earthly features like roads, waterbodies, etc. To make data analysis and forecasting easier, the TIFF format of satellite raster images must be preprocessed using ratio to generate the suitable .png format with appropriate band specification. The satellite images for this study were taken in the Kolar region of Karnataka.

Deep learning is an improvement over the simple neural network because it places more emphasis on the learning of successive "layers" of progressively more significant representations. The most used deep learning techniques in the field of agricultural drought assessment are ANN, CNN, Gradient Boosting Model (GBM), Support Vector Machine (SVM), and modified versions of these algorithms. It has slow convergence in some cases, which can be solved using bio-inspired algorithms.

The major goal of this work is to incorporate the significance of bio-inspired strategies for improving machine learning hyper-parameter tuning used for drought prediction. Using stochastic search approaches, bio-inspired algorithms can locate close to ideal answers to complex optimization problems. Sparrow Search Algorithm (SSA) and Barnacles Mating Optimizer (BMO) were chosen due to the accuracy and efficiency in their results compared to many other bio-inspired algorithms.

The drought prediction method proposed in this paper uses CNN and bio-inspired approaches that are based on satellite image indices. This is an extended work of our published papers (Sardar et al. 2022a; Sardar et al. 2022b).

The organization of the paper is as follows. Section II discusses the related work on the machine learning techniques for drought assessment. Section III explains the methodology for the vegetation indices calculation based on satellite image data, in addition to the design and development of a hybrid model based on deep learning techniques—convolutional neural networks (CNN) integrated with one of the SSAs and BMOs considering the indices as population. Section IV describes the results obtained in terms of accuracy, convergence time, and loss of three models (CNN, CNN integrated with SSA, and CNN integrated with BMO). Section V concludes the work done for drought assessment.

2. RELATED WORKS

Deep Learning techniques, such as Artificial Neural Networks (ANN), Convolutional Neural Networks (CNN), Gradient Boosting Models (GBM), Support Vector Machines (SVM), and modified versions of these algorithms, were primarily used in previous research conducted in the field of drought prediction. When analyzing drought using satellite images, drought indices, including the Normalized Vegetation Index (NDVI), Vegetation Condition Index (VCI), and Temperature Condition Index (TCI) were utilized. For future works, most authors mentioned improving the precision of their models and fusing them with other techniques for a more rapid, precise, and affordable implementation of the models. Studies on Barnacle Mating Optimizer (BMO) and Sparrow Search Algorithm (SSA) compared them with other recent algorithms, and they were found to yield good results. A conclusion could be drawn that these algorithms could be implemented into models for optimization purposes.

As per our previous work history, we started drought prediction with a CNN model using NDVI values computed from satellite images to predict and classify it using binary classifications (Sardar et al. 2021). The classes considered were drought or no drought. The CNN model was evaluated using the Nash Index, Root Mean Square Error (RMSE), and the correlation coefficient. Up to 96% improved accuracy was observed.

In continuation, we have used CNN variants for drought prediction such CNN, AlexNet, and VGGNet to compare and analyze the most suitable model (Chaudhari et al. 2021) considering deep learning and artificial intelligence advancement. Satellite images of a region and Normalized DVI, SAVI, EVI, and ARVI indices calculated from these are used. CNN was found to handle the image data with slightly better accuracy and very minimal loss as compared to the other models.

Agricultural drought traits that occur after meteorological droughts were evaluated, and the impact of meteorological droughts on agriculture and soil moisture for the Malaprabha sub-basin is observed (Sreekesh et al. 2019) based on Standard Precipitation Index (SPI), NDVI, TCI, VCI, Vegetation Health Index (VHI), and Temperature-Vegetation Dryness Index (TVDI). VHI was found to be more suitable for agricultural drought assessment.

A ground-based drought index – SPEI (Standardized Precipitation Evapotranspiration Index) was replicated by utilizing thirty remotely detected dry spell factors from the Tropical Rainfall Measuring Mission (TRMM) and the Moderate Resolution Imaging Spectroradiometer (MODIS) satellite sensors (Feng et al. 2019). The outcomes proposed that AI based remotely detected dry season checking is more appropriate for semi-parched and vegetation-delicate conditions.

Long-term drought prediction using a Deep Belief Network that consists of two restricted Boltzmann machines was proposed for the Gunnison River Basin region using a Standardized Streamflow Index (SSI) (Agana and Homaifar 2017a). The model was

compared with traditional methods like Support Vector Regression (SVR), and Multilayer Perceptron (MLP). When using Root Mean Square Error and Mean Absolute Error metrics, the model shows performance improvement.

A hybrid model using the Empirical Mode Decomposition (EMD) technique and a deep belief network was used for Long Term Drought Prediction (Agana and Homaifar 2017b). Various time scale dry spell indices throughout the Gunnison River Basin in the Upper Colorado River Basin are projected. Results have shown the improved performance in comparison to methods without series decomposition (MLP and DBN).

A strategy was devised for knowledge extraction from satellite images for drought monitoring utilizing NDVI values (Berhan et al. 2011). The use of near real-time spatio-temporal Meteosat Second Generation (MSG) data for drought monitoring in areas of Ethiopia with food insecurity was investigated.

Deep Forwarded Neural Networks (DFNN) with the Soil Moisture Deficit Index (SMDI) as a response variable was used to monitor drought with remote sensing data over South Asia (Prodhan et al. 2021). The model's performance was compared with Distributed Random Forest (DRF) and Gradient Boosting Machine (GBM), and it was found to outperform both for SMDI prediction.

Land Surface Temperature (LST), Evapo-Transpiration (ET), vegetation, and snow cover were considered using images of products from the MODIS sensor, rainfall using images from the TRMM satellite, and soil moisture using images from the SMOS satellite (Mokhtari and Mehdi 2021). ANN was found to give the best results when compared to SVR, Decision Tree, and Random Forest algorithms for predicting NDVI.

An experimental drought monitoring tool called VegOut-Ethiopia was developed in by Tadesse et al. (2014). A regression-tree technique was used to predict the values of NDVI for Ethiopia. The correlation coefficients were found to be between 0.5 to 0.9 for predicted and satellite-observed vegetation conditions.

The use of Remote Sensing (RS) and Geographic Information System (GIS) was emphasized for drought risk evaluation (Himanshu et al. 2015). The study aimed to recognize the relationship between rainfall and NDVI by integrating satellite, meteorological, and other ancillary data. The results found a strong linear relationship between NDVI and precipitation.

Strategies to converge remote sensing and supervised learning (SL) techniques were proposed by Kruseman et al. (2019). SPI is considered as a measure for drought analysis. Results obtained were satisfactory for predicting meteorological indices.

New strategies were devised for agricultural drought mapping with classification and regression trees (CART), boosted regression trees (BRT), random forests (RF), multivariate adaptive regression splines (MARS), flexible discriminant analysis (FDA), and support vector machines (SVM) (Rahmati et al. 2020). Relative departure of soil moisture (RDSM) was calculated for southeast Queensland. The RF model was found to be the most

accurate and FDA to be the least.

An ANN-based drought forecasting approach was used to predict quantitative values of Effective Drought Index (EDI) and SPI (Morid 2007). The Southern Oscillation Index (SOI) and North Atlantic Oscillation (NAO) climate indices were used. The study area was the Tehran Province of Iran. Various ANN models were tested for EDI and SPI and were compared.

A novel swarm optimization algorithm, Sparrow Search Algorithm (SSA), inspired by the sparrows' foraging, cooperative behavior, and anti-predator instincts was presented by Xue and Shen (2020). A set of 19 benchmark functions were used to evaluate SSA's performance. The results were compared with Grey Wolf Optimization (GWO), Particle Swarm Optimization (PSO), and Gravitational Search Algorithm (GSA), and SSA was found to outperform them.

A Learning Sparrow Search Algorithm solves the shortcomings of SSA's randomness and falling into local optimum (Ouyang et al. 2021). It introduces the lens reverse learning strategy in the algorithm's discovery stage, and a differential based local search. The Learning SSA algorithm is compared with Chaotic SSA, SSA, Brain Storm Optimizer (BSO), Grey Wolf Optimizer (GWO), and Particle Swarm Optimizer (PSO).

A new evolutionary optimization algorithm named Barnacles Mating Optimizer (BMO) is inspired by the natural behavior of barnacles during mating (Sulaiman et al. 2018a; 2018b). A set of 23 mathematical functions are utilized to evaluate the characteristics of BMO in finding the best solutions, particularly in unimodal, multimodal, and composite test functions. Results showed that BMO produced competitive results or outperformed the Genetic Algorithm (GA), Particle Swarm Optimizer (PSO), Differential Evaluation (DE), Sparrow Search Algorithm (SSA), and Whale Optimization Algorithm (WOA) for the benchmark test functions.

It is observed that the related work used either machine learning or bio-inspired algorithms. This paper aims to develop hybrid models of machine learning and optimization algorithms. CNN is chosen as the machine learning algorithm, while SSA and BMO are chosen as the bio-inspired algorithms. The main contributions are as follows.

1. Development of CNN model for computation of vegetation indices based on satellite images. Satellite images are preprocessed and converted from TIFF format to .png format before applying CNN for indices computation. Computed indices include Normalized Difference Vegetation Index (NDVI), Atmospherically Resistant Vegetation Index (ARVI), and Soil Adjusted Vegetation Index (SAVI).
2. Development of a CNN model for drought assessment using the calculated indices.
3. Development of a hybrid model that integrates developed CNN with bio-inspired algorithms – SSA (Sardar et al. 2022a) and BMO (Sardar et al. 2022b). A bio-inspired algorithm provides the initial weights to the CNN model. Initial population is taken from computed indices.

4. Performance analysis of the CNN model, and both hybrid models, for drought assessment in terms of accuracy, loss, and convergence time.
5. Design and development of a multi-class classification model for predicted drought.

3. PROPOSED HYBRID MODEL FOR DROUGHT ASSESSMENT

The proposed drought assessment includes various components as shown in Figure 1. Satellite images are collected from the ISRO (Indian Space Research Organization) satellite in the Kolar region of Karnataka from the National Remote Sensing Center (NRSC) and stored in a satellite image database component. The satellite images are supplied in TIFF format and require preprocessing for conversion to .png format. The CNN model components take a .png satellite image as an input to automatically analyze its features. Based on analyzed features, the computing indices component computes the vegetation indices, which are stored in an Excel file as a database for further drought assessment. With the goal of increasing prediction accuracy and the efficiency of assessment, a hybrid model is developed for assessment of drought by using computed indices from the historical spatial data based on satellite images. A hybrid model is integrated with a CNN model with bio-inspired techniques: SSA and BMO.

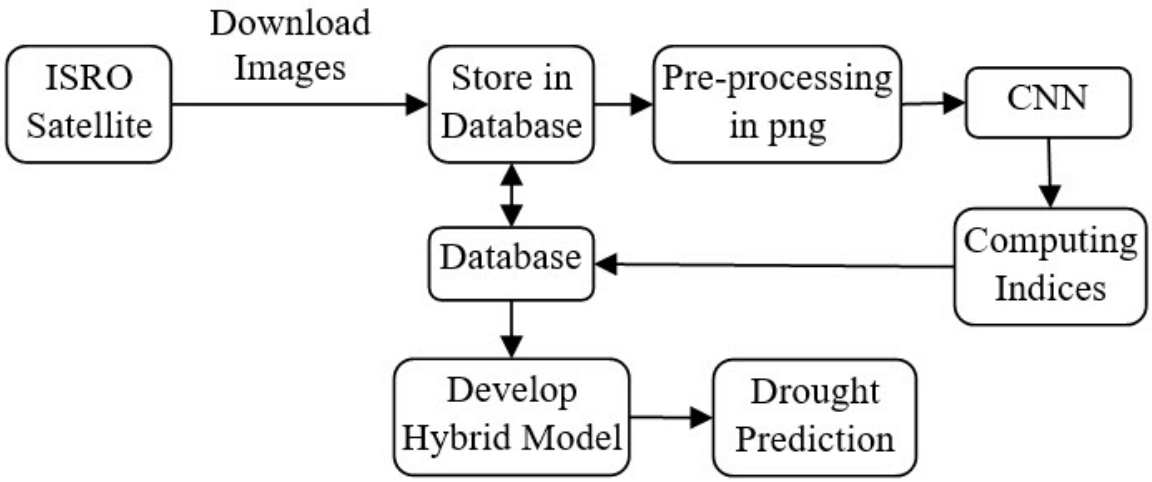

Figure 1 Components of hybrid model for drought assessment.

The initial results of these hybrid models are published in Sardar et al. 2022a and 2022b, respectively. The model is developed in Python, and the GPU is utilized to run the CNN and bio-inspired algorithms. The drought prediction component predicts the drought severity as a multi-class classification. The indices computation serves as the initial population for both the bio-inspired algorithms. There are six conventional functions F1()

to F6(). Performance of all is obtained, and F6 () is used in SSA, while the F3 () function is used in BMO to determine the fitness of each population, which is described in Section 4.

3.1 Hybrid model based on SSA for drought assessment

The hybrid model of CNN with SSA is designed as shown in Figure 2. The population is initialized with the calculated indices, as shown in Equation 1, and the standard F6 () function is used to calculate the fitness of the population. The best-fit population is chosen after 100 iterations, which is used as the initial weights in the input layer of the CNN model, making it a hybrid model. SSA has Discoverer, Follower, and Investigator phases, which are discussed in this section.

G: the maximum iterations= 100
PD: the number of producers=4
SD: the number of sparrows who perceive the danger = 4
R2: the alarm value = 0.2
n: the number of sparrows

Initialize a population of n sparrow as defined in Equation 4 and calculate the fitness values
while *(t<G)*
    Rank the fitness values and find the current best individual and the current worst individual
    R2=rand(1)
    for *i=1 : PD*
        Using Equation 1 update the sparrow location
    end for
    for *i=(PD+1):n*
        Using Equation 3 update the sparrow's location
    end for
    Get the current new location
    If the new location is better than before update it
    t=t+1
end while
return Xbest, fg

Figure 2 Pseudo code for SSA.

The Discoverer, as the name implies, looks for food, discovers food, and provides guidance to other community members. The location update formula for the Discoverer is shown in Equation 1.

$$X_{i,j}^{t+1} = \begin{cases} X_{i,j}^{t} \cdot exp\left(\dfrac{-h}{\alpha \cdot m}\right), if\ R_2 < ST, \\ X_{i,j}^{t} + Q \cdot L, if\ R_2 \geq ST. \end{cases} \quad (1)$$

Where:

$X_{i,j}^{t}$ and $X_{i,j}^{t+1}$ = j^{th} dimension at current iteration *t and t+1 related* to the *ith* sparrow,

α and *h* = random numbers between 0 and 1,

R_2 = alarm value between 0 and 1,

ST = safety threshold with a value between 0.5 and 1.0,

Q = random number following Normal distribution,

L = a matrix of 1 x *d,*

d = number of columns of population *X*, where each element of the matrix is 1, and

M = largest number of iterations and is a constant.

Following the Discoverer, Followers scour the area in and around their site for food. The location of Followers' updates is calculated using Equation 2.

$$X_{i,j}^{t+1} = \begin{cases} Q \cdot exp\left(\dfrac{X_{worst}^{t} - X_{i,j}^{t}}{i^2}\right), if\ i > \dfrac{n}{2}, \\ X_{P}^{t+1} + \left|X_{i,j}^{t} - X_{P}^{t+1}\right| \cdot A^{+} \cdot L, otherwise. \end{cases} \quad (2)$$

Where:

$X_{i,j}^{t}$ and X_{p}^{t+1} = the producer's optimal position in iteration *t* and *t+1*,

n = number of sparrows,

X_{worst} = current global location in the worst case,

A = *1 x d* dimension, with each element equal to 1 or -1, assigned randomly, and

A^{+} = $(AA^{T})^{-1}$

Individuals from the population are chosen at random to be Investigators. Sparrows will flee to a secure location when predators invade by sending out signals. Investigators usethe behavior formula as given in Equation 3.

$$X_{i,j}^{t+1} = \begin{cases} X_{best}^{t} + \beta \cdot \left| X_{i,j}^{t} - X_{best}^{t} \right|, if\ f_i \neq f_g, \\ X_{i,j}^{t} + K \cdot \left(\frac{\left| X_{i,j}^{t} - X_{worst}^{t} \right|}{(f_i - f_w) + \varepsilon} \right), if\ f_i = f_g. \end{cases} \quad (3)$$

Where:

X_{best}^{t} = current global optimal location,

β = step size control parameter. It is a random number following Normal distribution. Its mean and variance are 0 and 1, respectively.

K = random number between -1 and 1,

f_i = present sparrow's fitness value,

f_g = current global best-fitness value,

f_w = worst-fitness value, and

ϵ = the smallest constant, avoids zero-division error.

The best-fit population from SSA is used as the initial weights in the input layer of the CNN model.

3.2 Hybrid model based on BMO for drought assessment

The hybrid model of CNN with BMO is designed as shown in Figure 3. The population is initialized with the calculated indices, as shown in Equation 4, and the standard F3() function is used to calculate the fitness of the population. The best-fit population is chosen after 100 iterations. Initialization, selection, and generation of offspring are the three phases in BMO.

```
Set n: the number of sparrows =24
Set max_iterations=100
Initialize the population of barnacle Xi
Calculate the fitness of each barnacle
Sorting to locate the best result at the top of the population (T-the best solution)
while (l< max_iterations)
        Set the value of pl=7
        Selection using Equations 5 and Equation 6
        barnacle_d=randperm(n)
        barnacle_m=randperm(n)

        if selection of Dad and Mum ≤ pl
          for each variable
              Off spring generation using Equation 7
          end for
        else if selection of Dad and Mum > pl
          for each variable
              Off spring generation using Equation 8
          end for
        Bring the current barnacle back if it goes outside the boundaries
        Calculate the fitness of each barnacle
        Sort and update T if there is a better solution
         l=l+1
end while
return T
```

Figure 3 Pseudo code for BMO.

Initialization

The population vector of the barnacles, which are a potential source of solutions, has the form as shown in Equation 4.

$$X = \begin{matrix} \\ \begin{bmatrix} x_1^1 & x_1^2 & x_1^3 & x_1^4 \\ \vdots & \vdots & \vdots & \vdots \\ x_n^1 & x_n^2 & x_n^3 & x_n^4 \end{bmatrix} \end{matrix} \begin{matrix} \mathbf{NDVI} & \mathbf{SAVI} & \mathbf{EVI} & \mathbf{ARVI} \end{matrix} \tag{4}$$

Where:

n = number of population or number of barnacles.

The best solution up to this point is found at the top of vector *X*, after the initial evaluation of vector *X* is completed.

Selection

The selection procedure imitates barnacle behavior and is predicated on the following notions:

1. The selection is done randomly, as given in Equation 5 and Equation 6, but restricted to the length of barnacles' penises, denoted as *pl*.
2. Each barnacle may contribute its sperm as well as receive sperm from another barnacle, and each barnacle can only be fertilized by one barnacle at one time.
3. If at a certain point the selection process selects the same barnacle, it means that self-mating or self-fertilization has occurred.

$$barnacle\_d = randperm(n) \tag{5}$$

$$barnacle\_m = randperm(n) \tag{6}$$

Off-spring generation

The Hardy-Weinberg principle serves as the inspiration for the new offspring generation for BMO. To create the new offspring from the parents of the barnacle, the formulas as given in Equation 7 and Equation 8 are implied.

$$x_i^{N\_new} = px^N{}_{barnacle\_d} + qx^N{}_{barnacle\_m} \; for\, k \le pl \tag{7}$$

$$x_i^{N\_new} = rand() \times x^N{}_{barnacle\_m} \; for\, k > pl \tag{8}$$

Where:

N = number of control variables,
p = normal distributed random number,
q = 1 - p,
$X_i^{N\_new}$ = new barnacle generated at iteration t,
k = random number to generate offsprings, and
pl = penis length of the barnacle.

The best-fit population from BMO is used as the initial weights in the input layer of the CNN model.

4. RESULTS ANALYSIS

GoogleColab has been used to implement the Python notebooks needed to execute the model. The Deep Learning model is trained and constructed using TensorFlow GPUs. The

Indago module for numerical optimization is used in the proposed model to implement all the metaheuristic methods inspired by nature.

A loss function in machine learning is a metric for determining how well your ML model can forecast the actual result, or the ground truth. The output value of our model and the predicted value based on the ground truth will serve as the inputs for the loss function. The loss, which is a measurement of how well our model predicted the result, is the result of the loss function. When the loss was high, the model did not perform well. A low loss number indicates that our model performed effectively. The right loss function must be used to train an accurate model. Certain loss functions will have characteristics that will aid your model in learning a particular way. Some researchers could place greater importance on outliers than on the majority. In Table 1, a variety of losses that were seen during the experiment are displayed together with the computation method that was employed.

Table 1 Loss function formulas.

Loss function	Formula
Mean Squared Error (MSE)	$MSE = \frac{\sum_{i=1}^{n}\left(y_i - \hat{y}_i\right)^2}{n}$
MAE – Mean Absolute Error	$MAE = (1/n) * \sum \lvert y_i - x_i \rvert$
MSLE – Mean Squared Logarithmic Error	$MSLE = \frac{1}{n}\sum_{i=1}^{n}\left(\log(Y_i) - \log(\hat{Y})\right)^2$
Huber loss	$L_\delta\left(y, f(x)\right) = \begin{cases} \frac{1}{2}\left(y - f(x)\right)^2 \; for \lvert y - f(x)\rvert \le \delta, \\ \delta\lvert y - f(x)\rvert - \frac{1}{2}\delta^2 \; otherwise \end{cases}$
KLD – Kullback-Leibler Divergence Loss	$D_{KL}(P \parallel Q) = \sum_{x \in X} P(x) \log\left(\frac{P(x)}{Q(x)}\right)$

Parameters such as y_i, $\hat{y}_i$, n, δ, P, Q, X, and x are computed as part of the proposed algorithm and used for computation of these losses. Where X is sample data of size of n and given as an input to the proposed algorithm, x is the tuple in X, y_i is *ith* ground truth value to be predicted by the proposed algorithm, $\hat{y}_i$ is *ith* predicted value by the proposed algorithm, δ is the threshold value computed internally, P is the probability distribution, and Q is the reference probability distribution.

In this paper, we have combined the CNN model with two bio-inspired techniques and observed promising results. The model was trained using the spatial images and corresponding indices data for a particular region. The time taken for training has reduced impressively when combined with both the bio-inspired techniques, as

shown in Table 2. The time taken for Epoch 1 is 16 s, whereas the time taken for the hybrid model is far less. This is considered as convergence time of the hybrid algorithms in this paper. For the CNN model, the time taken for Epoch 1, and time taken for Epoch 2 is 16 s (3 s/step), and 2 s (2 s/step), respectively. For the CNN integrated with SSA model, it is found to be 3 s (3 s/step) and 0 s (43 ms/step), respectively. For the CNN integrated with BMO model, it is found to be 3 s (2 s/step) and 0 s (46 ms/step) respectively.

Table 2 Comparison of algorithms used for drought prediction.

Drought Prediction Model	Time Taken (Epoch1)	Time Taken (Epoch2)
CNN	16s 3s/step	2s 2s/step
CNN with SSA	3s 3s/step	0s 43ms/step
CNN with BMO	3s 2s/step	0s 46ms/step

CNN model only

For the CNN model, the training accuracy is below 90%; but during testing, the accuracy of the model is found to be 91%. Figure 4(a) shows the CNN model accuracy during training and testing. The model loss is shown in Figure 4(b). The loss is found to be higher during the model training. We can see that the model loss decreased to less than 0.1 during testing.

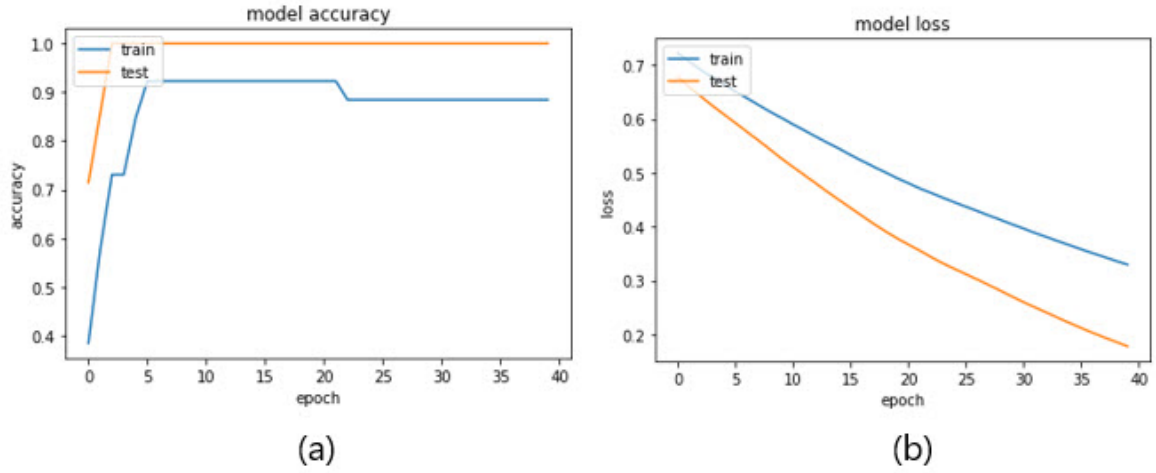

Figure 4 CNN model accuracy and loss.

CNN with SSA model

The hybrid model of CNN with SSA showed improved results for accuracy and model loss. All six fitness functions' accuracy and losses are given in this section.

F1 (): The accuracy shown in Figure 5(a) of the model during training is close to 85%. During testing of the model, the accuracy increased to 91%. The model loss shown in Figure 5(b) is high during training, close to 0.45, and it is close to 0.2 during the testing phase.

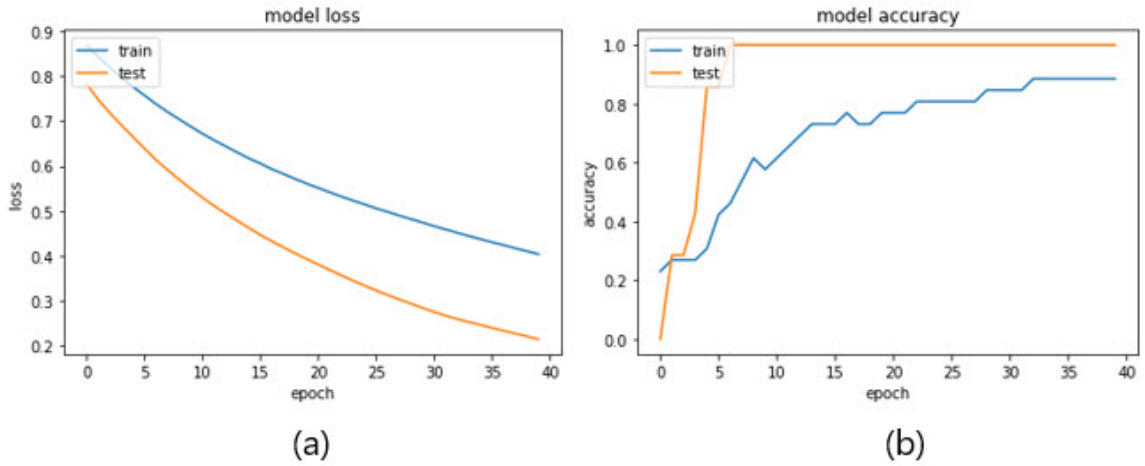

Figure 5 SSA hybrid model accuracy and loss – F1().

F2 (): The accuracy shown in Figure 6(a) of the model during training is close to 85%. During testing of the model, the accuracy increased to 88%. The model loss shown in Figure 6(b) is high during training, close to 0.40, and is close to 0.15 during the testing phase.

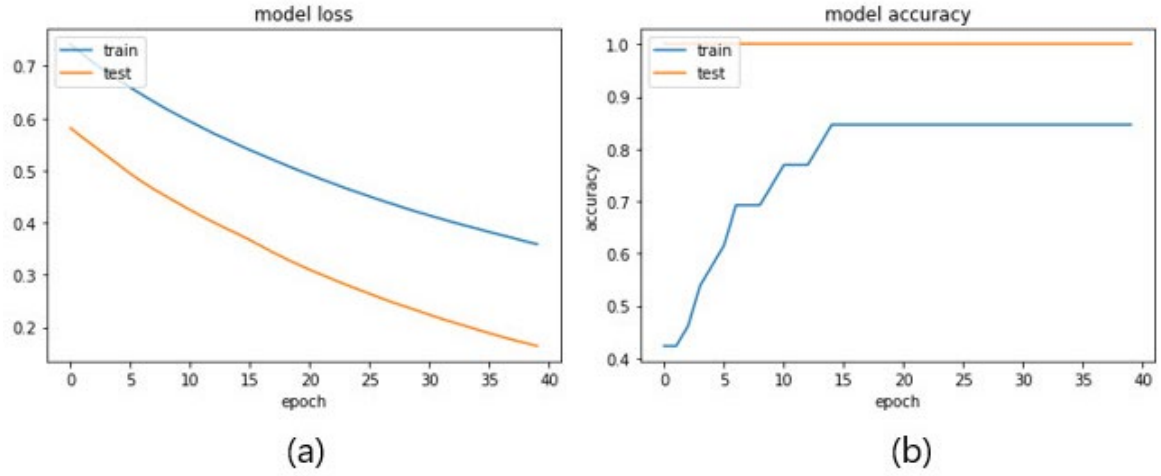

Figure 6 SSA hybrid model accuracy and loss – F2().

F3 (): The accuracy shown in Figure 7(a) of the model during training is close to 83%. During testing of the model, the accuracy increased to 92%. The model loss shown in Figure 7(b) is high during training, close to 0.45, and is close to 0.2 during the testing phase.

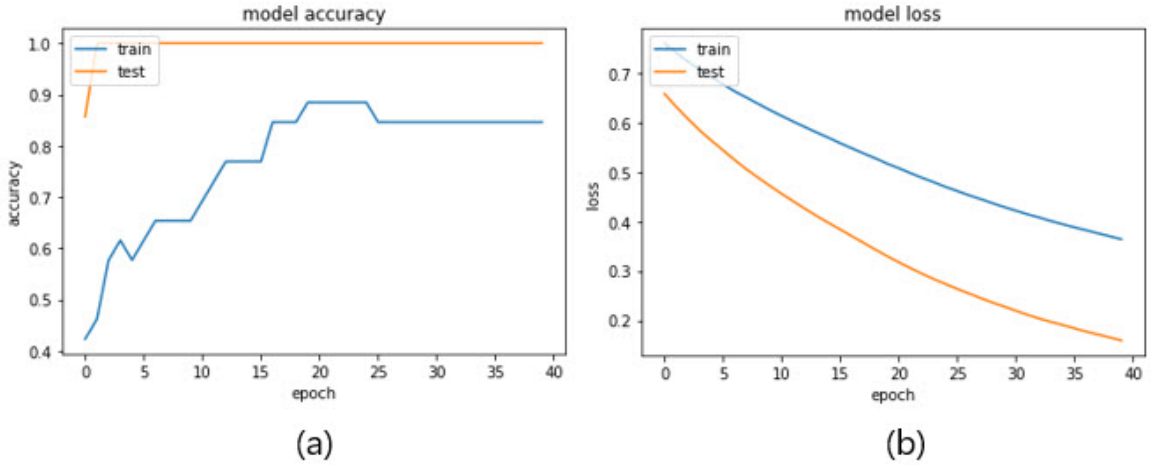

Figure 7 SSA hybrid model accuracy and loss – F3().

F4 (): The accuracy shown in Figure 8(a) of the model during training is close to 87.5%. During testing of the model, the accuracy increased to 91%. The model loss shown in Figure 8(b) is high during training, close to 0.35, and is close to 0.15 during the testing phase.

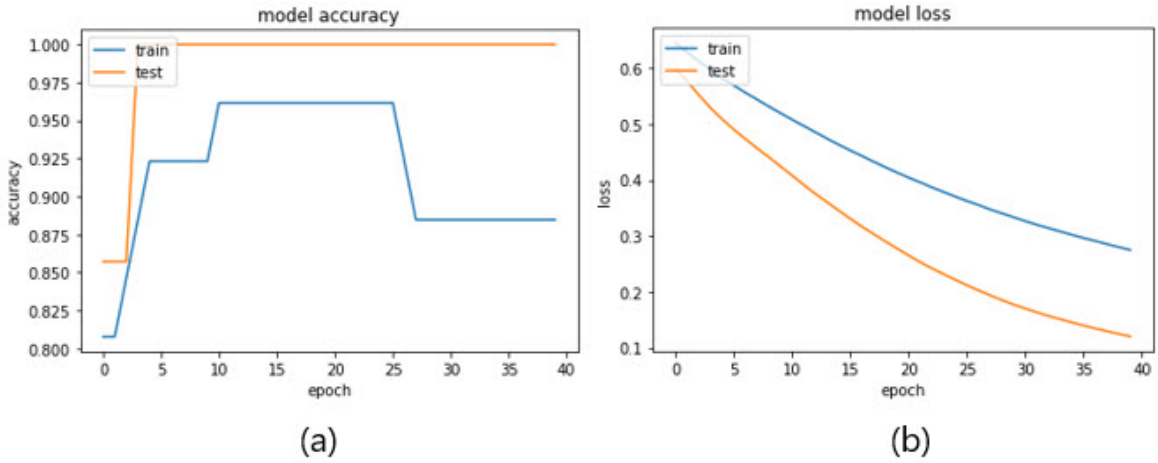

Figure 8 SSA hybrid model accuracy and loss – F4().

F5 (): The accuracy shown in Figure 9(a) of the model during training is close to 80%. During testing of the model, the accuracy increased to 91%. The model loss shown in Figure 9(b) is high during training, close to 0.35, and is close to 0.15 during the testing phase.

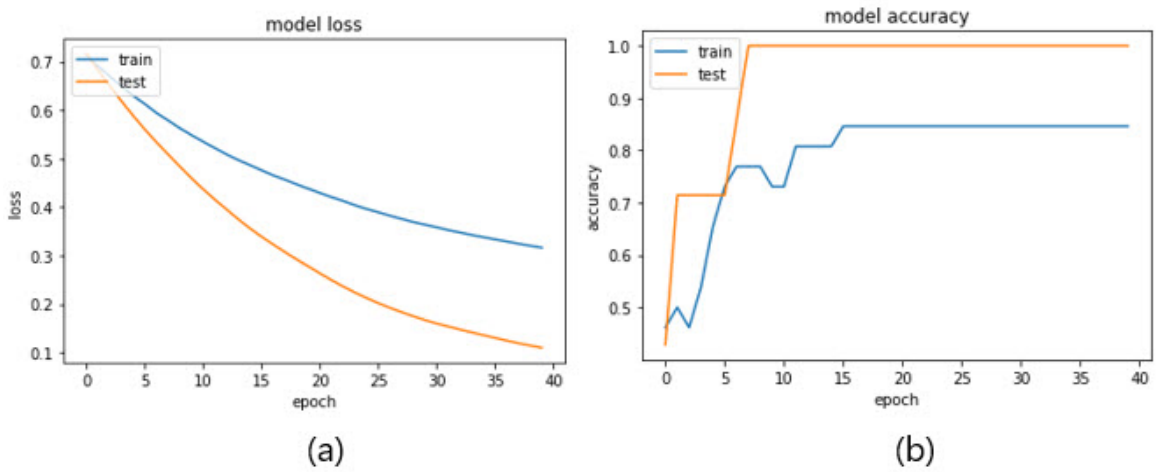

Figure 9 SSA hybrid model accuracy and loss – F5().

F6 (): The hybrid model of CNN with SSA showed improved results for accuracy, as shown in Figure 10(a), and model loss is shown in Figure 10(b). The accuracy of the model during training is close to 90%. During model testing, the accuracy increased to 94%. The hybrid model loss is similar to the model loss of CNN during the testing phase. The loss is found to be higher during model training, at 0.40. We can see that the model loss decreased to less than 0.15 during testing.

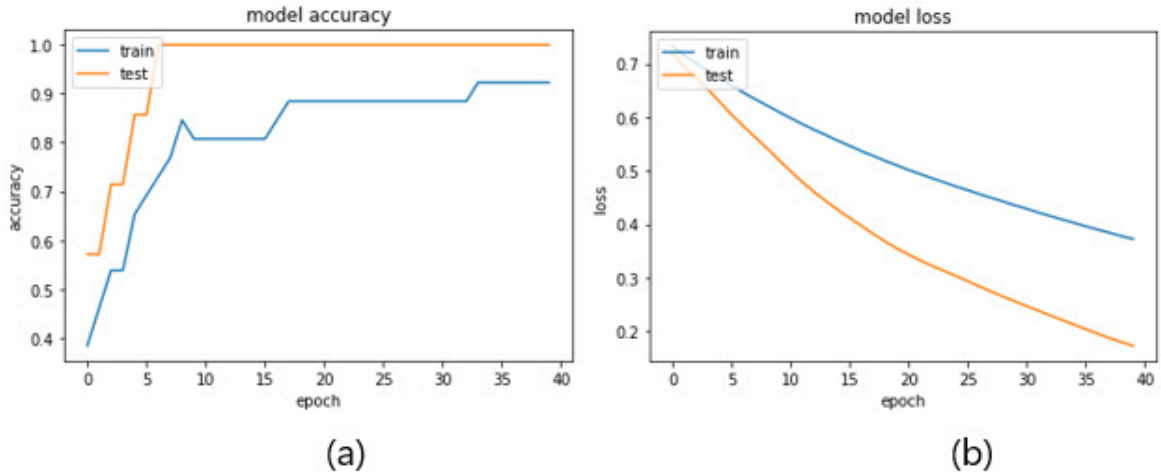

Figure 10 SSA hybrid model accuracy and loss – F6().

F6 is the only function where the accuracy reached 90% in the training phase.

Using all 6 fitness functions F1, F2, F3, F4, F5, F6 (SSA): We can see the F6 function shows the highest accuracy, as shown in Figure 11(a). F4 is first at a higher value, but then decreases below F6. F1, F2, and F3 show similar end points but F2 is lowest. F5 has the least accuracy among the functions. The accuracy graph is related to the training of the model. Model loss for F4 is the least, followed by F5 and F6. F1 has the highest model

loss, as shown in Figure 11(b), and thus is not a good option. F6 shows the best accuracy among other functions, while the loss is approximately 0.40, which is acceptable.

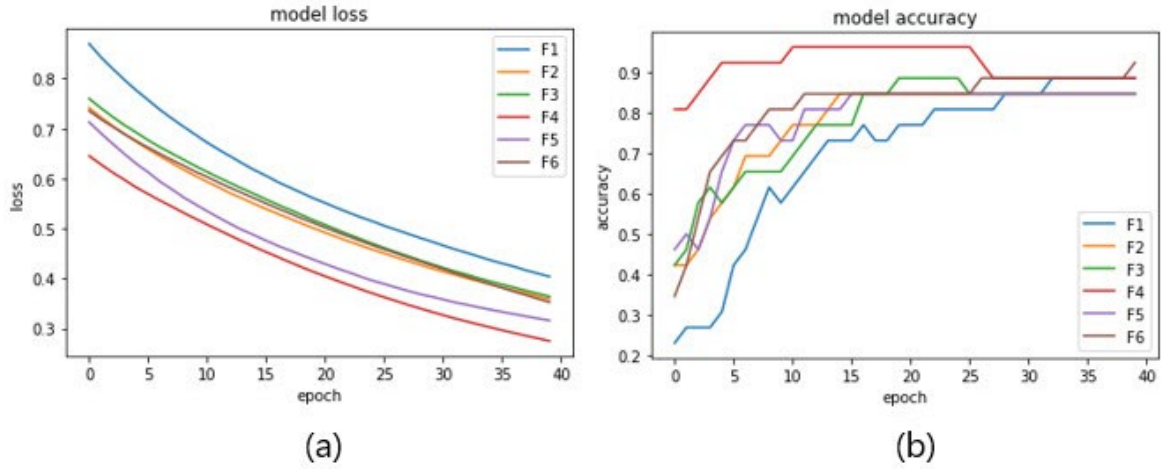

Figure 11 SSA hybrid model accuracy and loss.

Fitness functions (SSA)

The values (bio-weights) correspond to the best-fit population after 100 iterations, as shown in Figure 12. The population value (best-fit) for F2 is found to be the least. F6 is the next function and is found to have the best bio-weights for CNN [5.50, 5.5, 0, 5.50, and 5.50]. F4 is next, followed by F1 and F5. F3 has the highest values.

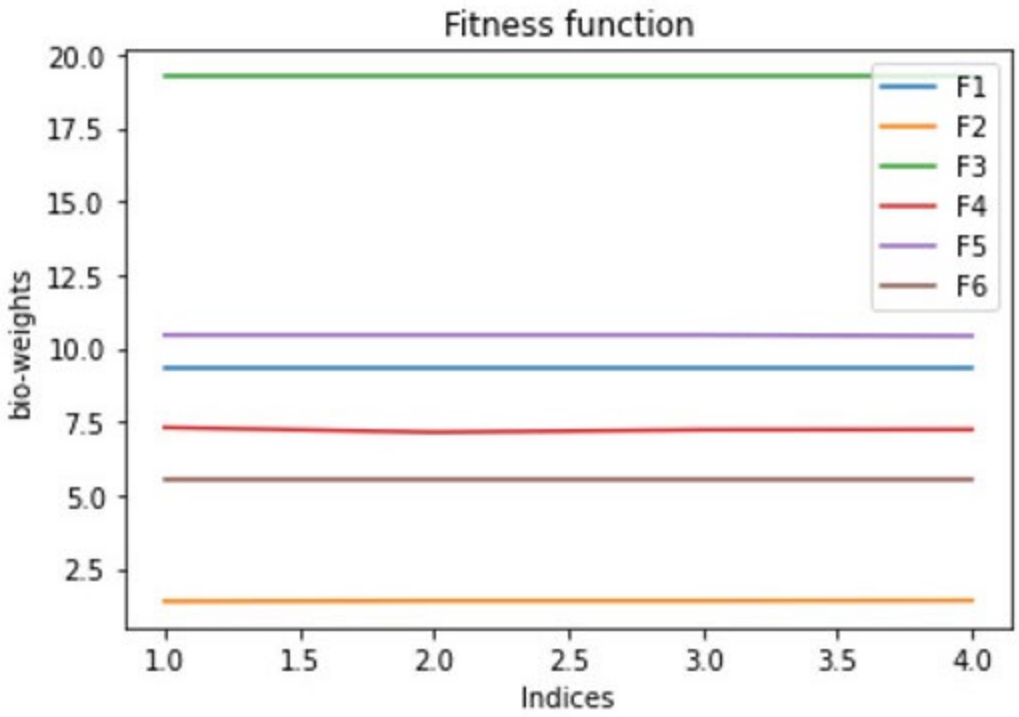

Figure 12 SSA-based hybrid model—bio-weights correspond to the best fit.

Accuracies of fitness functions (SSA)

The accuracy for each fitness function is shown in Figure 13. F1 is 0.91, F2 is 0.88, and F3, F4, and F5 are 0.91. F6 has the highest accuracy with 0.94.

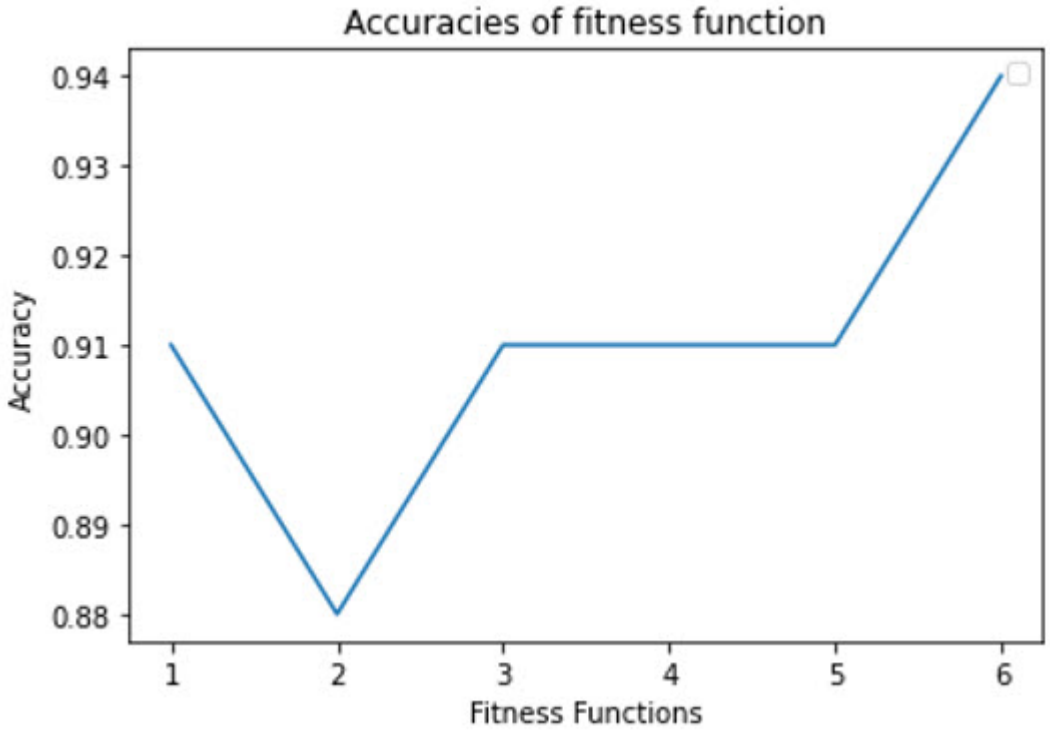

Figure 13 SSA-based hybrid model—fitness function accuracy.

SSA accuracy, loss, MSE loss, MAE loss, MSLE loss, Huber loss, and KLD loss are shown in Figure 14(a) through Figure 14(g), respectively. For the fitness functions F3 and F6, the MSE loss function has the least training loss, and the least testing loss, respectively. For MAE, fitness function F4 has the lowest training loss, and fitness function F3 has the lowest testing loss. Regarding MSLE, fitness function F1 has the lowest training loss, and the lowest testing loss. Fitness functions F1 and F6 have the lowest training and testing losses, respectively, for Huber loss. Fitness function F2 has the lowest testing loss, and the lowest fitness function F6 has the lowest training loss for the KLD loss function.

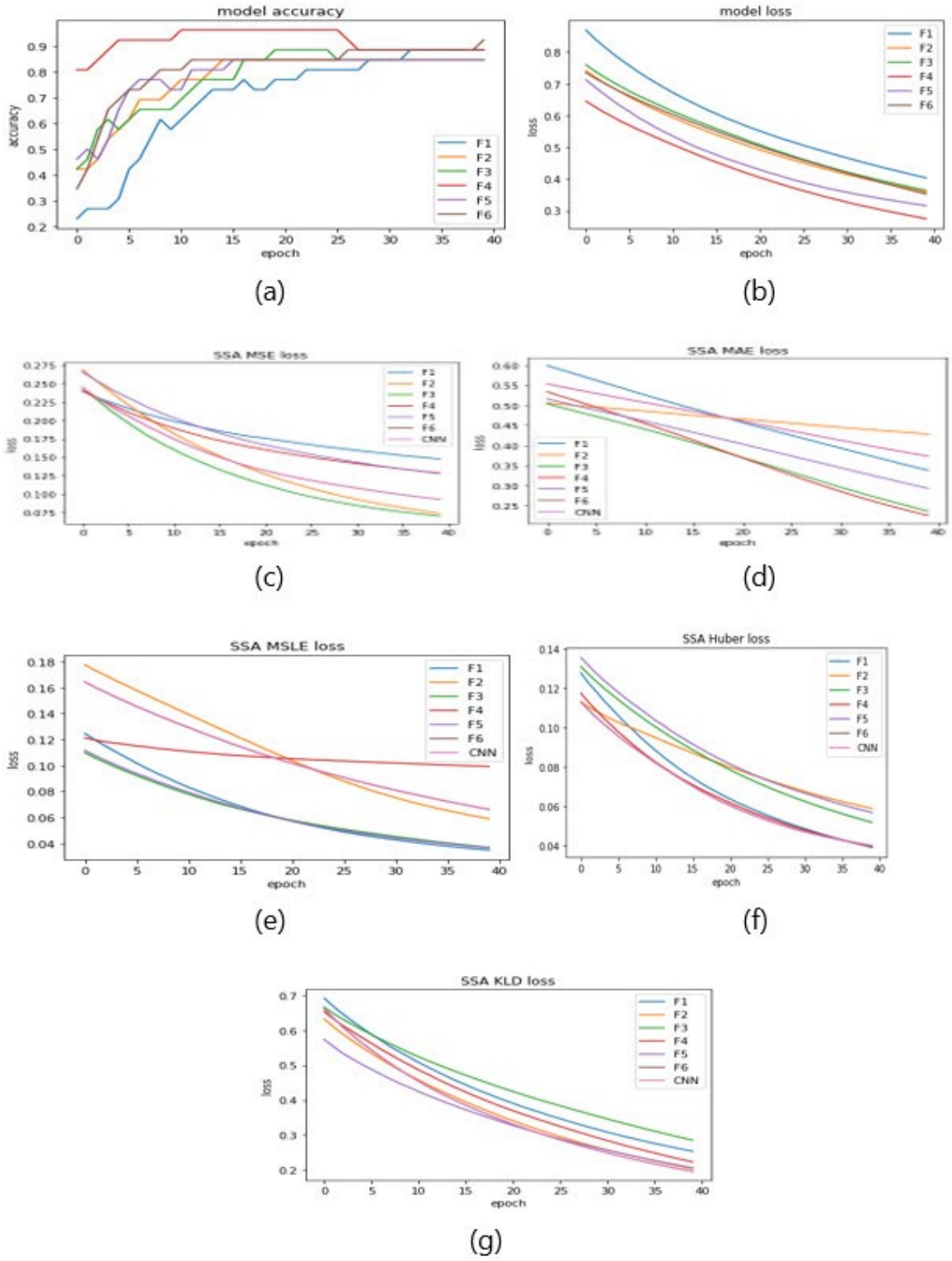

Figure 14 SSA accuracy and loss functions

4.1 CNN with BMO model

F1 (): The accuracy as shown in Figure 15(a) of the model during training is close to 88%. During testing of the model, the accuracy is increased to 91%. The model loss as shown in Figure 15(b) is high during training, close to 0.30, and is close to 0.10 during the testing phase.

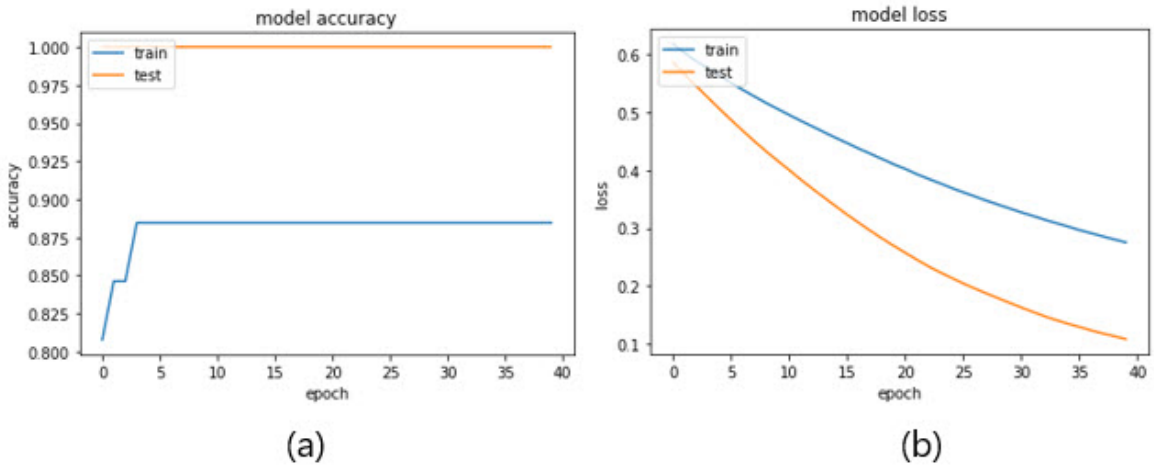

Figure 15 CNN-BMO model accuracy and loss – F1().

F2 (): The accuracy as shown in Figure 16(a) of the model during training is close to 85%. During testing of the model, the accuracy increased to 91%. The model loss as shown in Figure 16(b) is high during training, close to 0.35, and is close to 0.15 during the testing phase.

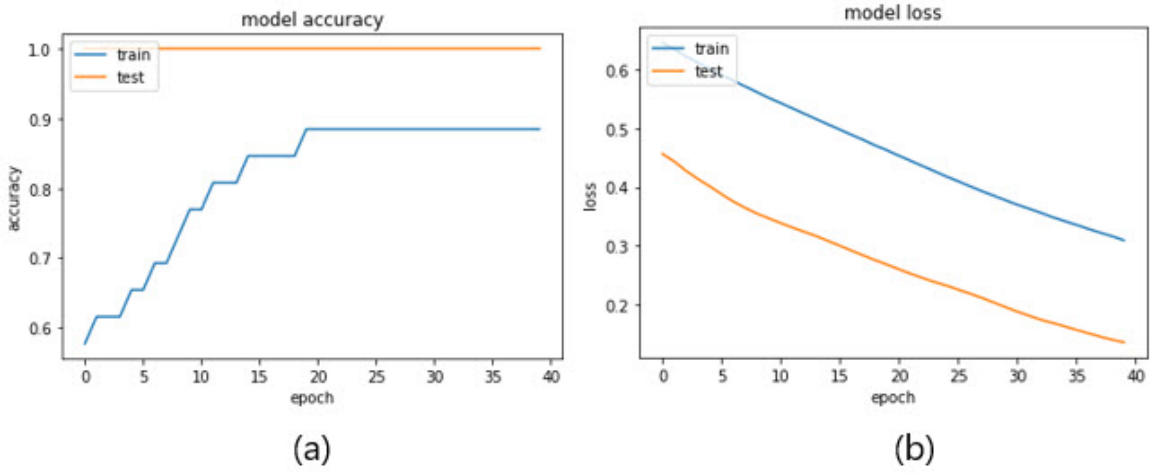

Figure 16 CNN-BMO model accuracy and loss – F2().

F3 (): The accuracy, as shown in Figure 17(a) of the model during training, is close to 92%. During testing of the model, the accuracy increased to 94%. The model loss as shown in

Figure 17(b) is high during training, close to 0.30, and is close to 0.20 during the testing phase. The accuracy using F3 is found to be the highest (94%).

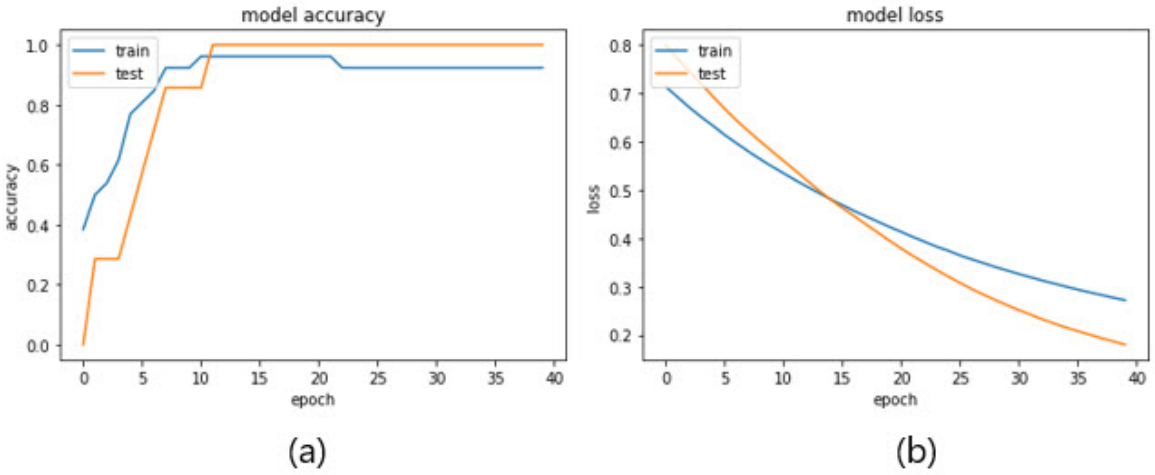

Figure 17 CNN-BMO model accuracy and loss – F3().

F4 (): The accuracy as shown in Figure 18(a) of the model during training is close to 85%. During testing of the model, the accuracy increased to 91%. The model loss as shown in Figure 18(b) is close to 0.45 during the training phase and is close to 0.2 during the testing phase.

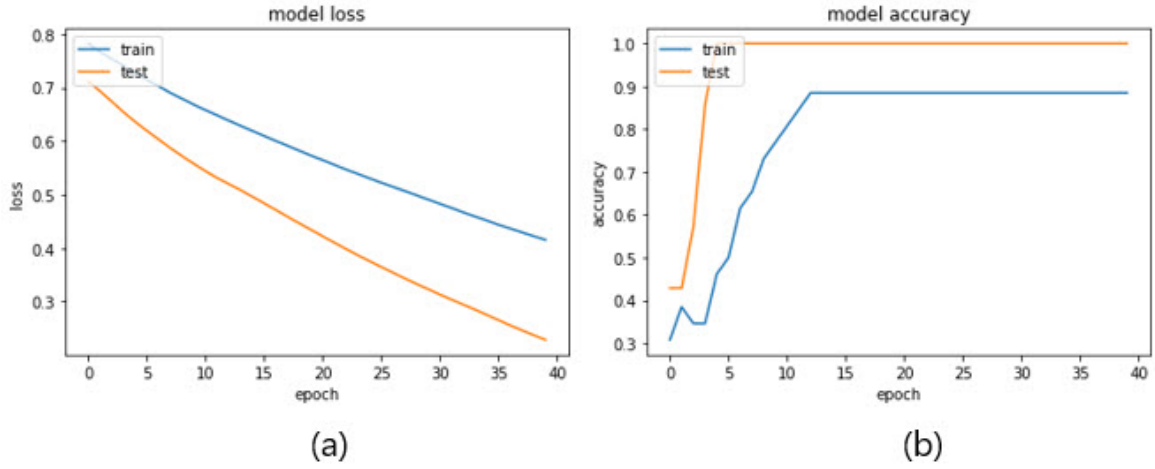

Figure 18 CNN-BMO model accuracy and loss – F4().

F5 (): The accuracy as shown in Figure 19(a) of the model during training is close to 85%. During testing of the model, the accuracy increased to 88%. The model loss as shown in Figure 19(b) is close to 0.40 during the training phase and is close to 0.2 during the testing phase.

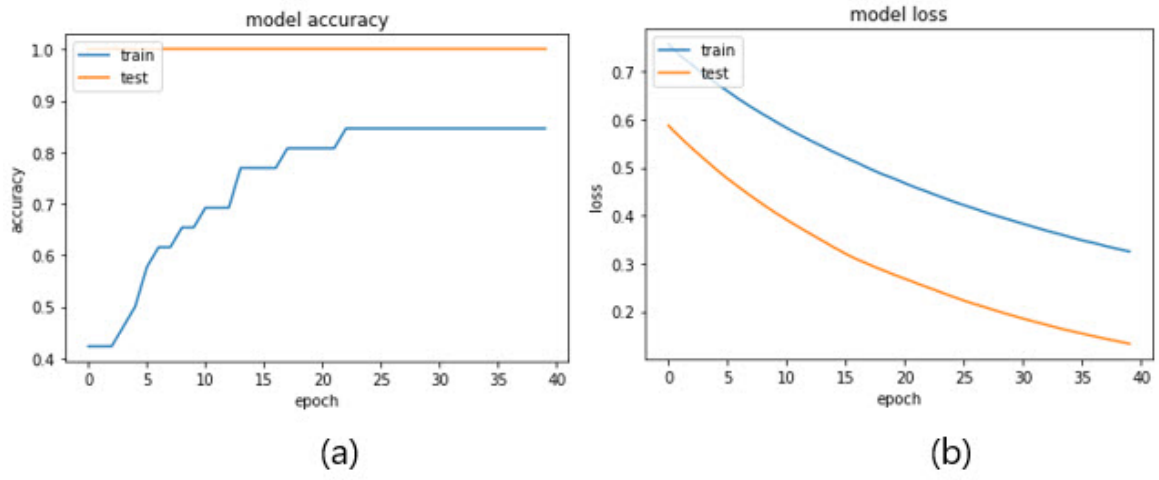

Figure 19 CNN-BMO model accuracy and loss – F5().

F6 (): The accuracy as shown in Figure 20(a) of the model during training is close to 85%. During testing of the model, the accuracy is 91%. The model loss as shown in Figure 20(b) is close to 0.50 during the training phase. During the testing phase, the model loss was high initially, but decreased after a certain number of epochs, close to 0.25.

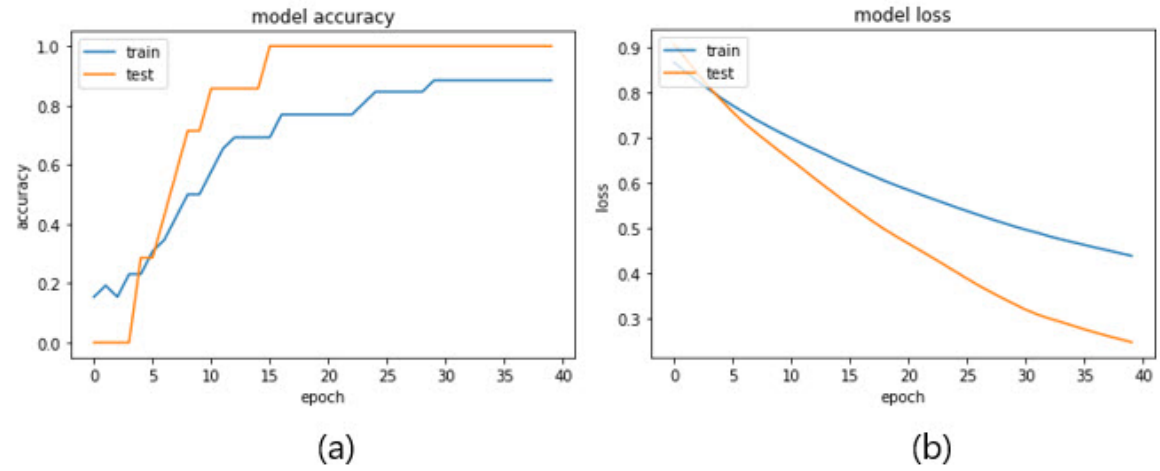

Figure 20 CNN-BMO model accuracy and loss – F6().

Using all 6 fitness functions, F1, F2, F3, F4, F5, F6 (): it is clear from Figure 21(a) that the F3 function is showing the highest accuracy. F1, F2, F4, F6 show similar end points. F5 has the least accuracy among the functions. The accuracy graph is related to the training of the model. Model loss as shown in Figure 21(b) is the smallest for F1 and F3. F2 has the next lowest loss, followed by F5, then F4. F6 has the highest model loss. F3 shows the best accuracy among other functions, while the loss is approximately 0.30, which is acceptable.

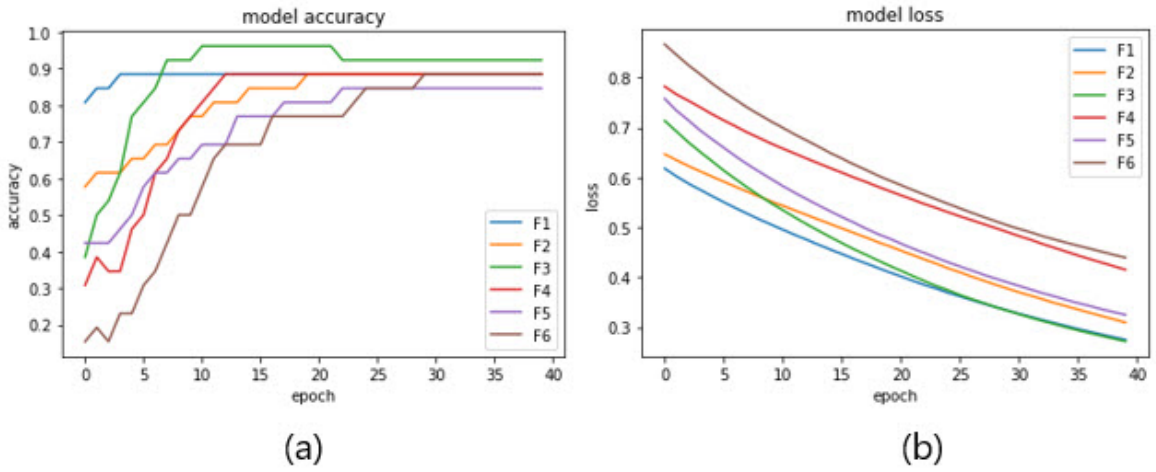

Figure 21 CNN-BMO hybrid model accuracy and loss.

Fitness functions: The values (bio-weights) correspond to the best-fit population after 100 iterations, as shown in Figure 22. The population value (best-fit) for F2 is found to be the lowest. F3 is next and is found to be the best bio-weights for CNN [5.77, 5.50, 5.77, and 5.77]. F1 is next, followed by F4 and F6. F5 has the highest values.

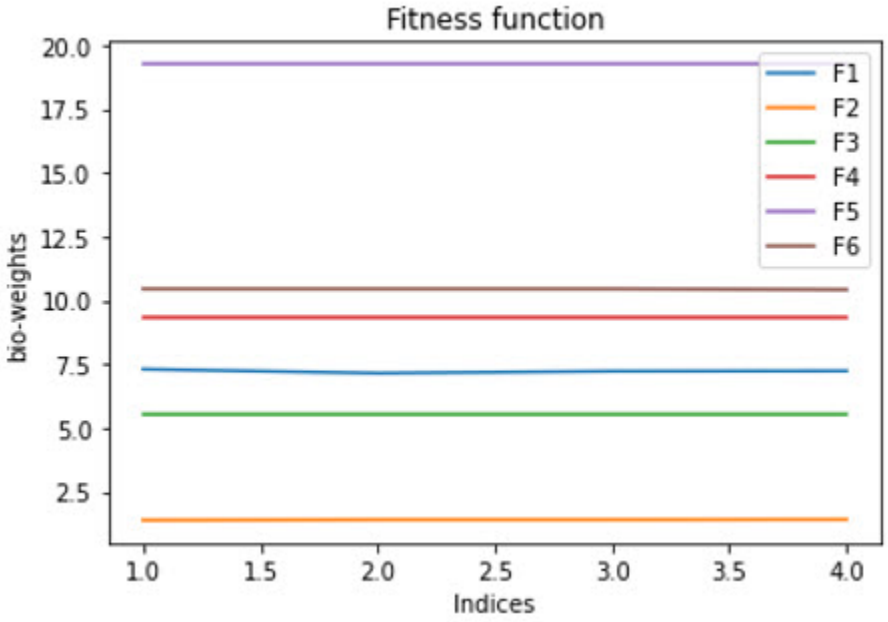

Figure 22 CNN with BMO model loss—best-fit bio-weights.

Accuracies of fitness functions (): Hybrid model final accuracies are shown in Figure 23 for each fitness function. F3 has 0.94, F5 has 0.88, while others have 0.91.

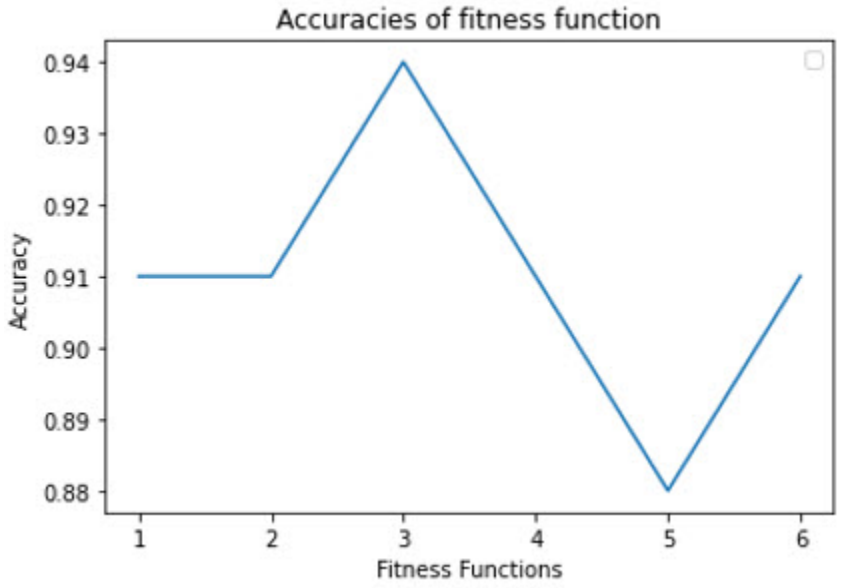

Figure 23 CNN with BMO model—fitness function accuracy.

BMO accuracy, loss, MSE loss, MAE loss, MSLE loss, Huber loss, KLD loss are shown in Figures 24(a– g), respectively. The MSE loss function has the lowest training loss and lowest testing loss for the fitness function F2, respectively. For MAE, the fitness function F5 has the lowest training loss, while the fitness function F6 has the lowest testing loss. Regarding MSLE, the fitness function F5 has the lowest training loss, and the lowest testing loss. The fitness function F1 has the lowest training loss, and the fitness function F5 has the lowest testing loss for Huber loss. In terms of the KLD loss function, the training loss and testing loss are both lowest for the fitness function F3.

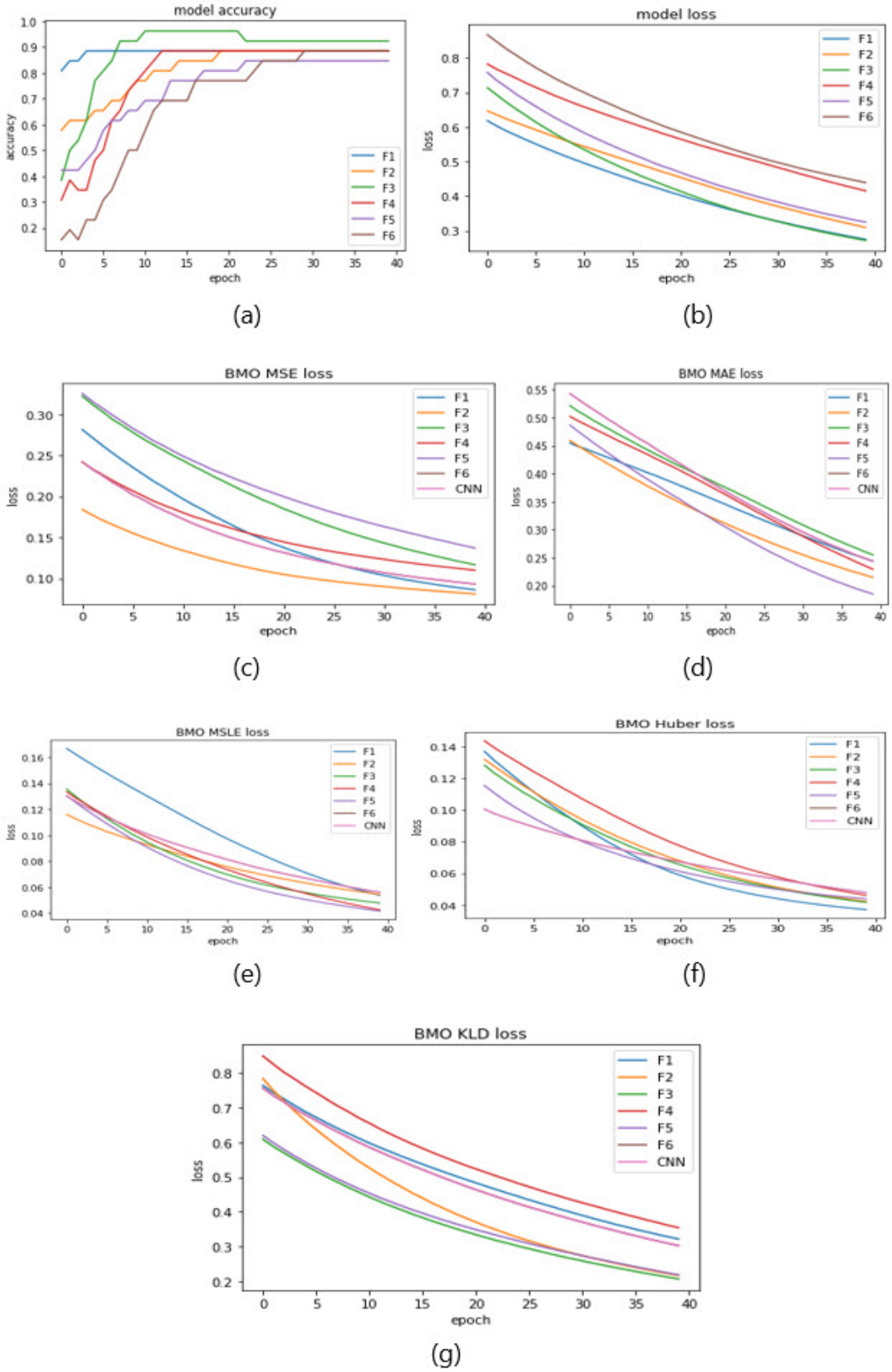

Figure 24 BMO accuracy and loss—all functions.

5 . CONCLUSION

In this paper, a hybrid model based on Convolutional Neural Networks (CNN) and two bio-inspired algorithms (SSA and BMO) to predict agricultural drought, using satellite images, is presented. The accuracy improved, while the time taken for training the hybrid model is found to be significantly reduced with the hybrid model, when compared to the standalone CNN model. For the CNN with SSA model, the accuracy is found to improve from 91% to 94%. The time taken for Epoch 1 is found to decrease from 16 s (3 s/step) to 3 s (3 s/step); for Epoch 2, it decreased from 2 s (2 s/step) to 0s (43 ms/step). For the CNN with BMO model, the accuracy is found to improve to 94%, the time for Epoch 1 decreased to 3 s (2 s/step), and the time for Epoch 2 decreased to 0 s (46 ms/step). For future research, other machine learning techniques could be employed, or a hybrid model based on different bio-inspired algorithms could be implemented with the goal of increasing the efficiency of the model even further.

REFERENCES

Agana, N.A., and A. Homaifar. 2017a. "A Deep Learning Based Approach for Long-Term Drought Prediction." SoutheastCon 2017, Concord, NC: 1–8.

Agana, N.A., and A. Homaifar. 2017b. "A Hybrid Deep Belief Network for Long-Term Drought Prediction." In *Proceedings of the Workshop on Mining Big Data in Climate and Environment* (MBDCE 2017): 27–29.

Berhan, G., H. Shawndra, T. Tsegaye, and A. Solomon. 2011. "Using Satellite Images for Drought Monitoring: A Knowledge Discovery Approach." *Journal of Strategic Innovation and Sustainability* 7 (1): 135–153.

Chaudhari, S., V. Sardar, D.S. Rahul, M. Chandan, M.S. Shivakale, and K.R. Harini. 2021. "Performance Analysis of CNN, AlexNet and VGGNet Models for Drought Prediction using Satellite Images." *2021 Asian Conference on Innovation in Technology (ASIANCON)*, PUNE, India, 1–6.

Feng, P., B. Wang, D.L. Liu, and Q. Yu. 2019. "Machine Learning-based Integration of Remotely-sensed Drought Factors can Improve the Estimation of Agricultural Drought in South-Eastern Australia." *Agricultural Systems* 173: 303–316.

Himanshu, S.K., G. Singh, and N. Kharola. 2015. “Monitoring of Drought Using Satellite Data.” *International Research Journal of Earth Sciences* 3 (1): 66–72.

Kruseman, G., L. Ornella, and J. Crossa. 2019. “Satellite Data and Supervised Learning to Prevent the Impact of Drought on Crop Production: Meteorological Drought.” In *Drought-Detection and Solutions.* IntechOpen: 85471.

Mokhtari, R., and A. Mehdi. 2021. "Data Fusion and Machine Learning Algorithms for Drought Forecasting using Satellite Data." *Journal of the Earth and Space Physics* 46 (4): 231–246.

Morid, S, V. Smakhtin, and K. Bagherzadeh. 2007. “Drought forecasting using artificial neural networks and time series of drought indices.” *International Journal of Climatology* 27: 2103–2111.

Ouyang, C., D. Zhu, and F. Wanq. 2021. “A Learning Sparrow Search Algorithm.” *Hindawi Computational Intelligence and Neuroscience* 2021, 3946958.

Prodhan, F.A., J. Zhang, F. Yao, L. Shi, T.P.P. Sharma, D. Zhang, D. Cao, M. Zheng, N. Ahmed, and H.P. Mohana. 2021. "Deep learning for monitoring agricultural drought in South Asia using remote sensing data." *Remote Sensing* 13 (9): 1715.

Rahmati, O., F. Falah, K.S. Dayal, R.C. Deo, F. Mohammadi, T. Biggs, D.D. Moghaddam, S.A. Naghibi, and D.T. Bui. 2020. "Machine Learning Approaches for Spatial Modeling of Agricultural Droughts in the South-east Region of Queensland Australia. "*Science of The Total Environment* 699, 134230.

Sardar, V.S., K.M. Yindumathi, S.S. Chaudhari, and P. Ghosh. 2021. "Convolution Neural Network-based Agriculture Drought Prediction using Satellite Images." IEEE Mysore Sub Section International Conference (MysuruCon), 601–7.

Sardar, V., S. Chaudhari, A. Anchalia, A. Kakati, A. Paudel, and B.N. Bhavana. 2022a. "Intelligent Hybrid Model for Drought Assessment Coupled with Bio-inspired Techniques.” IEEE 2nd Mysore Sub Section International Conference (MysuruCon), 1–6.

Sardar, V., S, Chaudhari, A. Anchalia, A. Kakati, A. Paudel, and B.N. Bhavana. 2022b. "Ensemble Learning with CNN and BMO for Drought Prediction.” In *IEEE 3rd Global Conference for Advancement in Technology (GCAT*), 1–6.

Sreekesh, S., N. Kaur, and S.R. Sreerama Naik. 2019. "Agricultural drought and soil moisture analysis using satellite image-based indices." *The International Archives of the Photogrammetry, Remote Sensing and Spatial Information Sciences*, XLII-3/W6, 507–514.

Sulaiman, M.H., Z. Mustaffa, M.M. Saari, H. Daniyal, I. Musirin, and M.R. Daud. 2018a. “Barnacles Mating Optimizer: An Evolutionary Algorithm for Solving Optimization.” IEEE International Conference on Automatic Control and Intelligence Systems, I2CACIS 2018, 99–104.

Sulaiman, M.H., Z. Mustaffa, M.M. Saari, H. Daniyal, M.R. Daud, S. Razali, and A.I. Mohammed. 2018b. “Barnacle Mating Optimizer: A Bio-Inspired Algorithm for Solving Optimization Problems.” 19th IEEE/ACIS International Conference on Software Engineering, Artificial Intelligence, Networking and Parallel/Distributed Computing (SNPD): 265–270.

Tadesse, T., G.B. Demisse, B.Zaitchik, and T. Dinku. 2014. “Satellite‐Based Hybrid Drought Monitoring Tool for Prediction of Vegetation Condition in Eastern Africa: A Case Study for Ethiopia.” *Water Resources Research* 50 (3): 2176–90.